# Focus shaping of the radially polarized Bessel–Gauss beam with a sine-azimuthal variation wavefront

Xiumin Gao[1, 4], Dawei Zhang[1, 2*], Ting Mei[3], Rui Fu[4], Songlin Zhuang[1]

[1]Engineering Research Center of Optical Instrument and System,
 Ministry of Education and Shanghai Key Lab of Modern Optical System,
 University of Shanghai for Science and Technology,
 No. 516 JunGong Road, Shanghai 200093, China

[2]School of Electrical and Electronic Engineering, Nanyang Technological University,
 50 Nanyang Avenue, Singapore 639798, Singapore

[3]Laboratory of Nanophotonic Functional Materials and
 Devices Institute of Optoelectronic Materials and Technology,
 South China Normal University, Guangzhou 510631, China

[4]Electronics and Information College, Hangzhou Dianzi University,
 Hangzhou 310018, China

*Corresponding author: dwzhang@usst.edu.cn

Focusing properties of the radially polarized Bessel–Gauss beam with a sine-azimuthal variation wavefront was investigated by the vector diffraction theory. The wavefront distribution is the sine function of the azimuthal angle with one phase parameter that indicates the phase change frequency. Results show that the focal pattern can be altered by the phase parameter, and many novel focal patterns may occur, such as multiple dark-foci focal pattern, crescent shape, and wheel shape. For case of a higher phase beam, the whole focal pattern turns on a symmetric wheel shape with multiple reduplicate intensity elements. When the phase parameter is an odd number, the number of reduplicate elements equals the phase parameter, while when the phase parameter is an even number, the number of reduplicate elements is two times the phase parameter. In addition, the effect of the phase parameter on the focal pattern is more considerable than that of the beam parameter under low numerical aperture. Under higher numerical aperture, the effect of the beam parameter on the focal pattern gets stronger.

Keywords: Bessel–Gauss beam, wavefront modulation, vector diffraction theory.

## 1. Introduction

Since Durnin introduced Bessel beams in 1987, this kind of beams has attracted much attention for many potential applications [1–4]. However, ideal Bessel beams are not physically realizable because they carry infinite energy through any cross-section

normal to their propagation direction [5]. In order to break through this physical difficulty, Gori *et al.* introduced the Bessel–Gauss beams that are characterized by a Bessel function with a Gaussian envelope [6]. Since then, the Bessel–Gauss beam has become the focus of many studies and received considerable attention [7–12]. Ito and co-workers generated the higher order modes of vector Bessel–Gauss beams by using a spot defect mirror in an Nd:YAG laser cavity [13]. Wang *et al.* created the needle of longitudinally polarized light in vacuum using binary optics with incident vector Bessel–Gauss beams [14]. And then the design of the diffractive optical element for generating this kind of a needle was also proposed [15]. Yew and Sheppard examined the effect of tightly focusing a radially polarized beam with uniform, Gaussian, and Bessel–Gauss pupil functions, and found that the resulting FWHM (full-width half-maximum) is the smallest for the case of a uniform amplitude profile, while the Bessel–Gauss beam results in the largest FWHM. In addition, the Bessel–Gauss beam benefits the most from the use of an annulus [16]. Huang *et al.* investigated the intensity profiles in the focal plane of vector-vortex beams that are focused by a high numerical aperture lens obeying the Helmholtz condition [17].

On the other hand, the wavefront modulation of beams has also attracted much attention [18–22]. For instance, wavefront modulation was proposed to extend focal depth [19]. However, to the best of our knowledge, the focusing of radially polarized Bessel–Gauss beams with a sine-azimuthal variation wavefront has not been studied so far. The present paper is aimed at investigating numerically the focal pattern of the radially polarized Bessel–Gauss beam with a sine-azimuthal variation wavefront by the vector diffraction theory. The principle of the focusing radially polarized Bessel–Gauss beam is given in Section 2. Section 3 shows the simulation results and discussions. The conclusions are summarized in Section 4.

## 2. Principle of focusing the radially polarized Bessel–Gauss beam with wavefront modulation

In the focusing system we investigated, the focusing beam is a radially polarized Bessel–Gauss beam whose amplitude of a transverse optical field is the same as that of the scalar Bessel–Gauss [14, 16], and its wavefront is the function of an azimuthal angle. Therefore, in the cylindrical coordinate systems $(r, \varphi, 0)$, the field distribution $\mathbf{E}(r, \varphi, 0)$ of the radially polarized Bessel–Gauss beam in the incident pupil plane is written as,

$$\mathbf{E}(r, \varphi, 0) = E_0(r, \varphi, 0) \cdot \mathbf{n}_r \tag{1}$$

where $\mathbf{n}_r$ is the radial unit vector of polarized direction. Wavefront phase distribution is chosen as the sine function of an azimuthal angle, namely $\phi = -\pi \sin(m\varphi)$. Term $E_0(r, \varphi, 0)$ is the optical field value distribution and can be written in the form [14, 16],

$$E_0(r, \varphi) = J_1\left(\frac{2\beta_1 \sin(\theta)}{\sin(\alpha)}\right) \exp\left[-\left(\frac{\beta_2 \sin(\theta)}{\sin(\alpha)}\right)^2\right] \exp\left[-i\pi \sin(m\varphi)\right] \tag{2}$$

where $\beta_1$ and $\beta_2$ are the beam parameters of Bessel–Gauss beams, and $\beta_1$ is called the Bessel beam parameter due to its relation to the Bessel function in this article. Parameter $\alpha$ is the half-angle of the convergence angle of the focusing optical system. Parameter $m$ is the phase parameter that indicates the phase change frequency. According to the vector diffraction theory, the electric field in the focal region of the radially polarized Bessel–Gauss beam is [16, 23],

$$\mathbf{E}_0(\rho, \phi, z) = E_\rho \mathbf{e}_\rho + E_\phi \mathbf{e}_\phi + E_z \mathbf{e}_z \tag{3}$$

where $\mathbf{e}_\rho$, $\mathbf{e}_\phi$, and $\mathbf{e}_z$ are the unit vectors in the radial, azimuthal, and propagating directions, respectively. To indicate the position in image space, cylindrical coordinates $(\rho, \phi, z)$ with the origin $\rho = z = 0$ located at the paraxial focus position are employed. $E_\rho$, $E_\phi$, and $E_z$ are the amplitudes of the three orthogonal components and can be expressed as [23, 24]

$$E_\rho(\rho, \phi, z) = \frac{-iA}{\pi} \int_0^\alpha \int_0^{2\pi} \sqrt{\cos(\theta)}\, E_0 \sin(\theta)\cos(\theta)\cos(\varphi - \phi) \times$$
$$\times \exp\left\{ik\left[z\cos(\theta) + \rho\sin(\theta)\cos(\varphi - \phi)\right]\right\} \mathrm{d}\varphi \mathrm{d}\theta \tag{4}$$

$$E_\phi(\rho, \phi, z) = \frac{-iA}{\pi} \int_0^\alpha \int_0^{2\pi} \sqrt{\cos(\theta)}\, E_0 \sin(\theta)\cos(\theta)\sin(\varphi - \phi) \times$$
$$\times \exp\left\{ik\left[z\cos(\theta) + \rho\sin(\theta)\cos(\varphi - \phi)\right]\right\} \mathrm{d}\varphi \mathrm{d}\theta \tag{5}$$

$$E_z(\rho, \phi, z) = \frac{iA}{\pi} \int_0^\alpha \int_0^{2\pi} \sqrt{\cos(\theta)}\, E_0 \sin^2(\theta) \times$$
$$\times \exp\left\{ik\left[z\cos(\theta) + \rho\sin(\theta)\cos(\varphi - \phi)\right]\right\} \mathrm{d}\varphi \mathrm{d}\theta \tag{6}$$

where $\theta$ denotes the tangential angle with respect to the $z$ axis, $A$ is one constant, $\varphi$ is the azimuthal angle with respect to the $x$ axis, and $k$ is the wave number. In order to make focusing properties clear and simplify the calculation process, after simple derivation, Eq. (2) can be rewritten as,

$$E_0(\theta, \varphi) = J_1\left(\frac{2\beta_1 \sin(\theta)}{\mathrm{NA}}\right) \exp\left[-\left(\frac{\beta_2 \sin(\theta)}{\mathrm{NA}}\right)^2\right] \exp\left[-i\pi \sin(m\varphi)\right] \tag{7}$$

where NA = $\sin(\alpha)$ under condition that the refractive index in the focal region is unit. By substituting Eq. (7) into Eqs. (4)–(6), we can obtain,

$$
E_\rho(\rho,\,\phi,\,z) \;=\; \frac{-iA}{\pi}\int_0^\alpha\int_0^{2\pi}\sqrt{\cos(\theta)}\,\sin(\theta)\cos(\theta)\cos(\varphi-\phi)\times
$$
$$
\times J_1\!\left(\frac{2\beta_1\sin(\theta)}{\mathrm{NA}}\right)\exp\!\left[-\left(\frac{\beta_2\sin(\theta)}{\mathrm{NA}}\right)^2\right]\exp\!\left[-i\pi\sin(m\varphi)\right]\times
$$
$$
\times\exp\!\left\{ik\!\left[z\cos(\theta)+\rho\sin(\theta)\cos(\varphi-\phi)\right]\right\}\mathrm{d}\varphi\,\mathrm{d}\theta
\tag{8}
$$

$$
E_\phi(\rho,\,\phi,\,z) \;=\; \frac{-iA}{\pi}\int_0^\alpha\int_0^{2\pi}\sqrt{\cos(\theta)}\,\sin(\theta)\cos(\theta)\sin(\varphi-\phi)\times
$$
$$
\times J_1\!\left(\frac{2\beta_1\sin(\theta)}{\mathrm{NA}}\right)\exp\!\left[-\left(\frac{\beta_2\sin(\theta)}{\mathrm{NA}}\right)^2\right]\exp\!\left[-i\pi\sin(m\varphi)\right]\times
$$
$$
\times\exp\!\left\{ik\!\left[z\cos(\theta)+\rho\sin(\theta)\cos(\varphi-\phi)\right]\right\}\mathrm{d}\varphi\,\mathrm{d}\theta
\tag{9}
$$

$$
E_z(\rho,\,\phi,\,z) \;=\; \frac{iA}{\pi}\int_0^\alpha\int_0^{2\pi}\sqrt{\cos(\theta)}\,\sin^2(\theta)\times
$$
$$
\times J_1\!\left(\frac{2\beta_1\sin(\theta)}{\mathrm{NA}}\right)\exp\!\left[-\left(\frac{\beta_2\sin(\theta)}{\mathrm{NA}}\right)^2\right]\exp\!\left[-i\pi\sin(m\varphi)\right]\times
$$
$$
\times\exp\!\left\{ik\!\left[z\cos(\theta)+\rho\sin(\theta)\cos(\varphi-\phi)\right]\right\}\mathrm{d}\varphi\,\mathrm{d}\theta
\tag{10}
$$

The optical intensity in the focal region is proportional to the modulus square of Eq. (3). It should be noted that when the phase parameter $m = 0$, namely, $E_0$ is not the function of the azimuthal angle $\varphi$, Eq. (5) and Eq. (9) are equal to zero. Basing on the above equations, focusing properties of radially polarized Bessel–Gauss beams can be investigated theoretically in detail.

## 3. Numerical results and discussions

Without loss of validity and generality, the beam parameter $\beta_2$ that relates to the Gaussian pupil distribution is chosen as a unit. The beam parameter $\beta_1$ that relates to the Bessel function is studied intensively because this parameter can alter the amplitude field very considerably. In order to explain the results of this article more clearly, we firstly show the wavefront distributions under condition of different phase parameters. Figure 1 illustrates wavefront distributions of the incident radially polar-
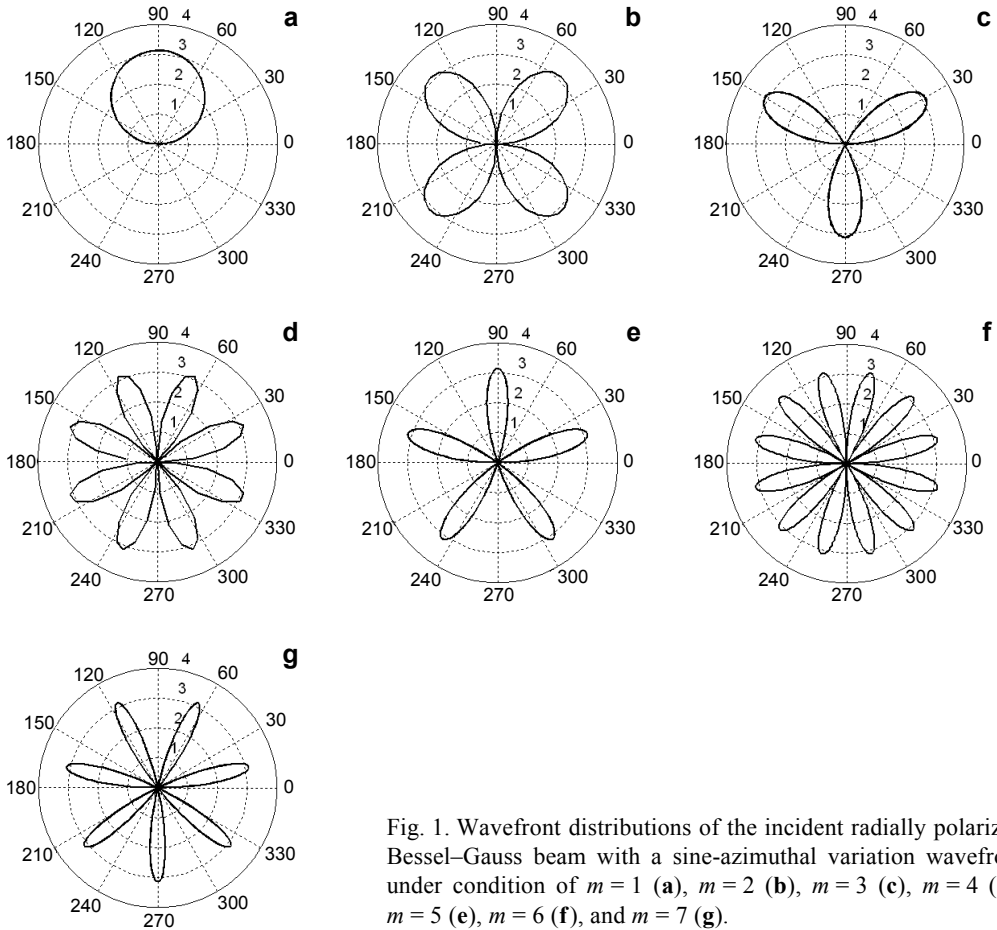
Fig. 1. Wavefront distributions of the incident radially polarized Bessel–Gauss beam with a sine-azimuthal variation wavefront under condition of $m = 1$ (**a**), $m = 2$ (**b**), $m = 3$ (**c**), $m = 4$ (**d**), $m = 5$ (**e**), $m = 6$ (**f**), and $m = 7$ (**g**).

ized Bessel–Gauss beam with a sine-azimuthal variation wavefront on the increasing phase parameter $m$. The polar coordinates are chosen in two dimensions, the azimuthal angle is in degrees, and the radial coordinate is the phase radian.

Now the focal patterns were studied in detail. Firstly, the intensity distributions in the focal plane under condition of $\beta_1 = 1$, NA = 0.5, and different phase parameters $m$ were studied. It should be noted that the distance unit in all figures is the wavelength of an incident beam in vacuum. There is only one annular focus with minimum center intensity for $m = 0$, namely there is no wavefront phase modulation, which is corresponding to the focal pattern of radially polarized beams under condition of lower numerical aperture. On increasing the phase parameter, the focal pattern changes very considerably. The annular focal pattern evolves into one crescent shape when the phase parameter increases from zero to unit, as shown in Fig. 2**b**. The focal pattern turns on a very symmetric focal pattern with five dark hollow foci with four outward Y-shape intensity spots under condition of $m = 2$, as shown in Fig. 2**c**. When $m$ increases to 3,
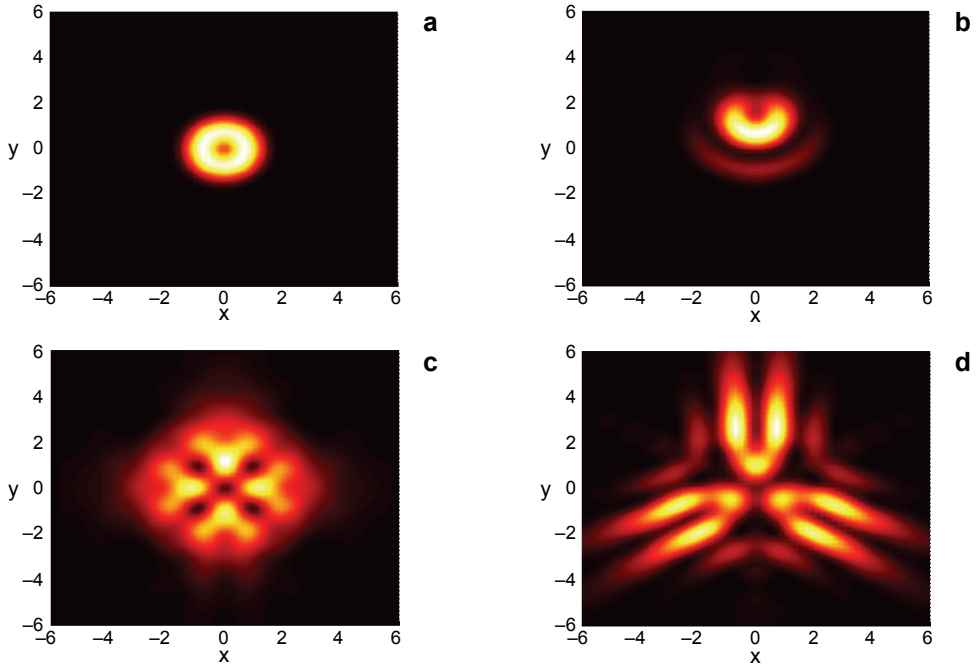
Fig. 2. Intensity distributions for $\beta_1 = 1$, NA = 0.5, and $m = 0$ (**a**), $m = 1$ (**b**), $m = 2$ (**c**), $m = 3$ (**d**).
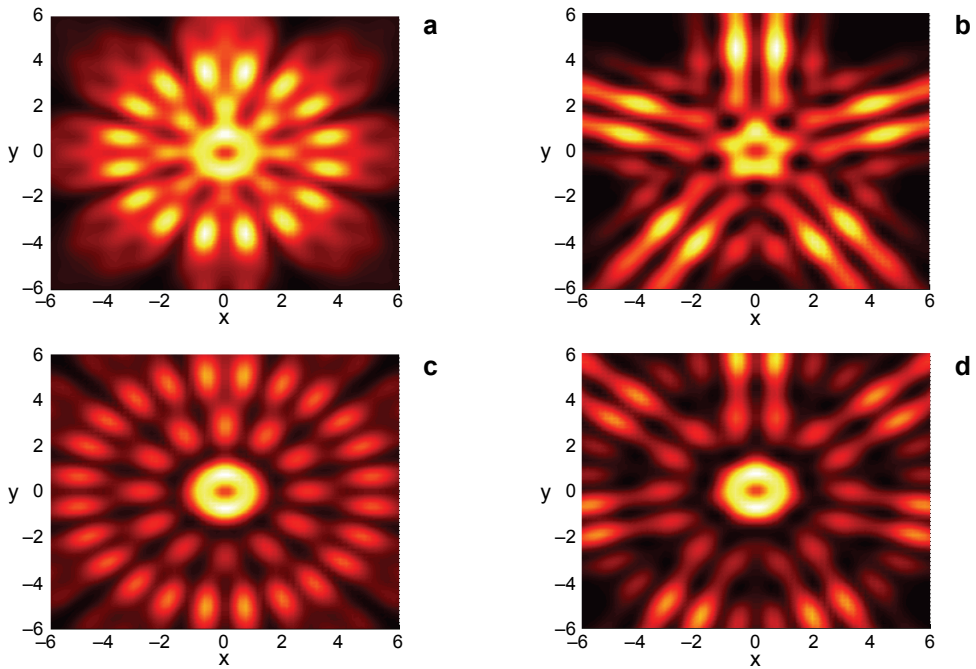


Fig. 3. Intensity distributions for $\beta_1 = 1$, NA = 0.5, and $m = 4$ (**a**), $m = 5$ (**b**), $m = 6$ (**c**), $m = 7$ (**d**).

the focal pattern extends and changes into three V-shape intensity peaks with angles pointing to the center, which leads to the whole triangle focal pattern.

When $m$ increases continuously, the whole focal pattern becomes more and more symmetric, and is very similar to a wheel consisting of multiple intensity peaks. There are eight Y-shape intensity peaks outside the center annular focal spot, which leads to the appearance of a wheel shape focal pattern, as shown in Fig. 3**a**. When the phase parameter $m$ is equal to five, the whole focal pattern changes into a pentagon, and each angle of the whole focal pattern consists of two main parallel intensity lines, as shown in Fig. 3**b**. For case of $m = 6$, the whole focal pattern changes into the wheel shape and the focal pattern consists of twelve Y-shape intensity peaks outside the center annular focal spot. And under condition of $m = 7$, the whole focal pattern changes into a seven angle shape, and each angle consists of two parallel intensity lines, as shown in Fig. 3**d**. From the above focal pattern evolution, we can see that the focal patterns can be altered considerably by a phase parameter, and many novel focal patterns have come into being. In addition, we also can see that when the phase parameter is an odd number, the focal pattern evolution on increasing phase parameter changes in a similar way, the angle number of the whole symmetric focal pattern is equal to the phase parameter, and each angle of the whole focal pattern consists of two parallel intensity lines. However, when the phase parameter is an even number, the angle number of the whole symmetric focal pattern is twice the phase parameter, and each angle of the whole focal pattern consists of one V-shape intensity peak. The above focal patterns may find applications in laser micro-machining and microscopy. It was usually deemed that in the optical trapping system, the forces exerted on the particle in the light field consist of two kinds of forces, one is the optical gradient force, which plays a crucial role in constructing an optical trap and its intensity is proportional to the optical intensity gradient; the other kind of force is scattering force, which usually has complex forms because this kind of force is related to the properties of trapped particles, and whose intensity is proportional to the optical intensity [25]. So, the peculiar intensity distribution in the focal region means that the controllable optical trap may occur. Though this paper is aiming at investigating the focusing of the radially polarized Bessel–Gauss beam, and shows that some peculiar intensity distributions may find application in optical trapping, we also think whether there are any other specific effects apart from the peculiar intensity distribution. What is more interesting and important, some other optical characteristics may also affect optical trapping, for example orbital angular momentum and optical field singularity, which is also encouraging us to get deep insight into the effect of the peculiar optical field, though now we do not obtain corresponding results. In addition, the focal patterns obtained in this paper may also be developed as one of the methods of measuring phase parameters of the kind of wavefront.

Here, the Bessel beam parameter is chosen as $\beta_1 = 2$, Figs. 4 and 5 illustrate the intensity distributions in the focal plane under condition of low numerical aperture NA = 0.5 and different phase parameters $m$. By comparing the focal patterns for case of $\beta_1 = 2$ with those for $\beta_1 = 1$, we can see that entire focal patterns extend considerably
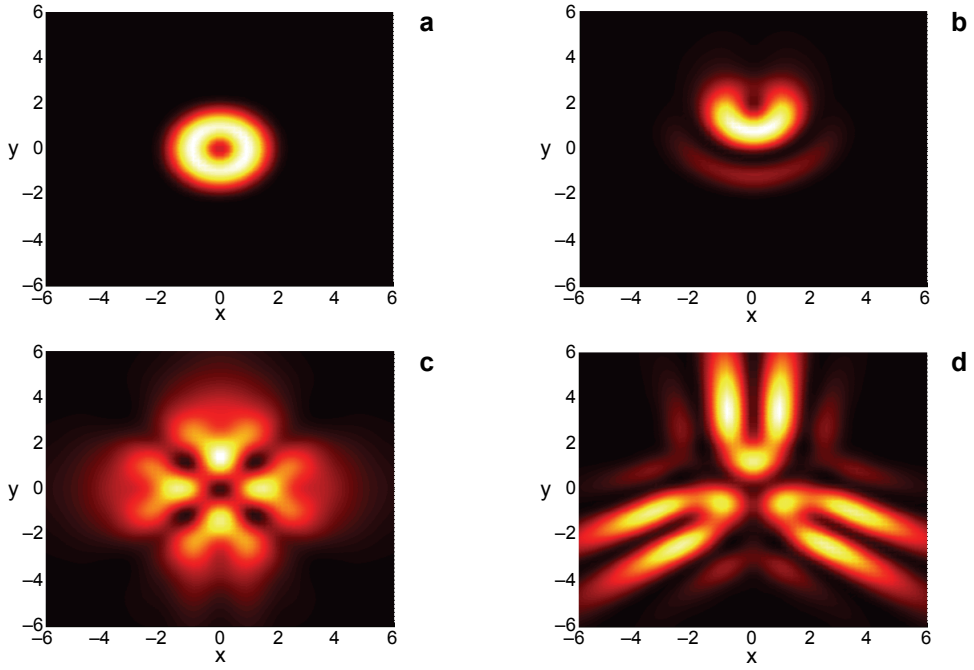
Fig. 4. Intensity distributions for $\beta_1 = 2$, NA = 0.5, and $m = 0$ (**a**), $m = 1$ (**b**), $m = 2$ (**c**), $m = 3$ (**d**).
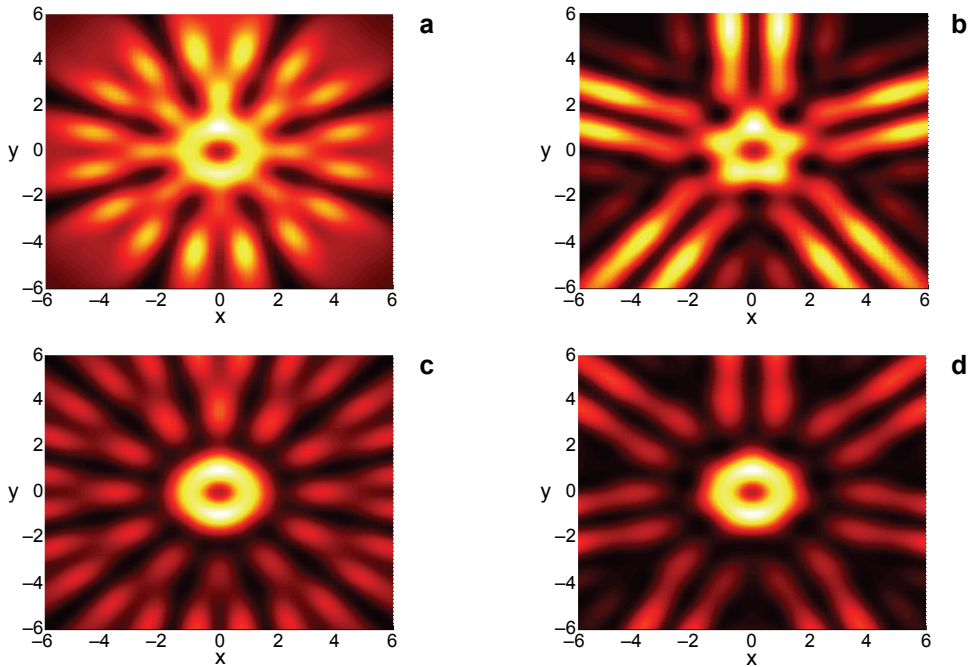


Fig. 5. Intensity distributions for $\beta_1 = 2$, NA = 0.5, and $m = 4$ (**a**), $m = 5$ (**b**), $m = 6$ (**c**), $m = 7$ (**d**).

for a higher Bessel beam parameter. The focal patterns for $\beta_1 = 0.2$ were also investigated and were shown in Figs. 6 and 7. The focal patterns evolution principle on increasing phase parameters $m$ and focal patterns for the same $m$ is very similar to those under condition of $\beta_1 = 2$ and $\beta_1 = 1$. Therefore, it can be seen that the effect of a phase parameter on the focal pattern is more considerable than the effect of the Bessel beam parameter $\beta_1$ under condition of the same low numerical aperture NA = 0.5.

Now we investigate the focal pattern evolution on an increasing phase parameter under condition of higher numerical aperture. Figures 8 and 9 illustrate the intensity distributions under condition of $\beta_1 = 1$, NA = 0.95, and different phase parameters $m$. There is only one intensity peak for $m = 0$, namely without any phase modulation, there is one spot in the focal region of the radially polarized Bessel–Gauss beam for higher numerical aperture, which is very familiar to those researchers who studied the focusing and application of radially polarized vector beams. When the phase parameter is one, the focal spot shifts along the $y$ coordinate, as shown in Fig. 8**b**. Under condition of $m = 2$, there are four main intensity peaks with four weak intensity peaks between them. When the phase parameter increases to 3, the whole focal pattern turns on a triangle shape where each reduplicate intensity element is dendritic, as shown in Fig. 8**d**. When the phase parameter $m$ increases continuously, the focal pattern changes considerably. Figure 9**a** shows the focal pattern for case of $m = 4$; there are eight reduplicate intensity elements, which construct a peak wheel. There are five reduplicate intensity elements under condition of $m = 5$, which leads to the focal
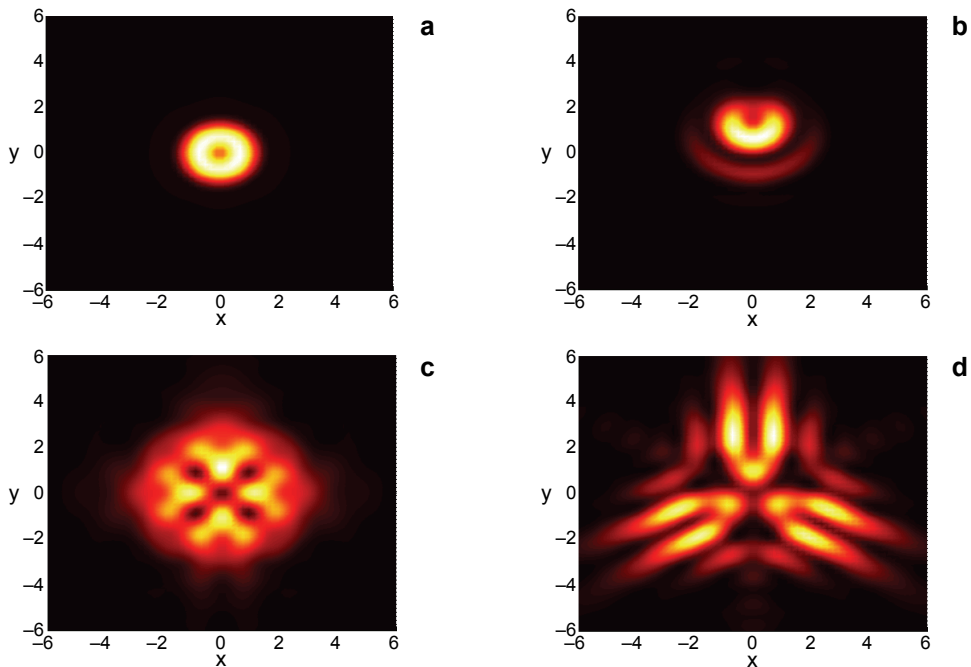


Fig. 6. Intensity distributions for $\beta_1 = 0.2$, NA = 0.5, and $m = 0$ (**a**), $m = 1$ (**b**), $m = 2$ (**c**), $m = 3$ (**d**).
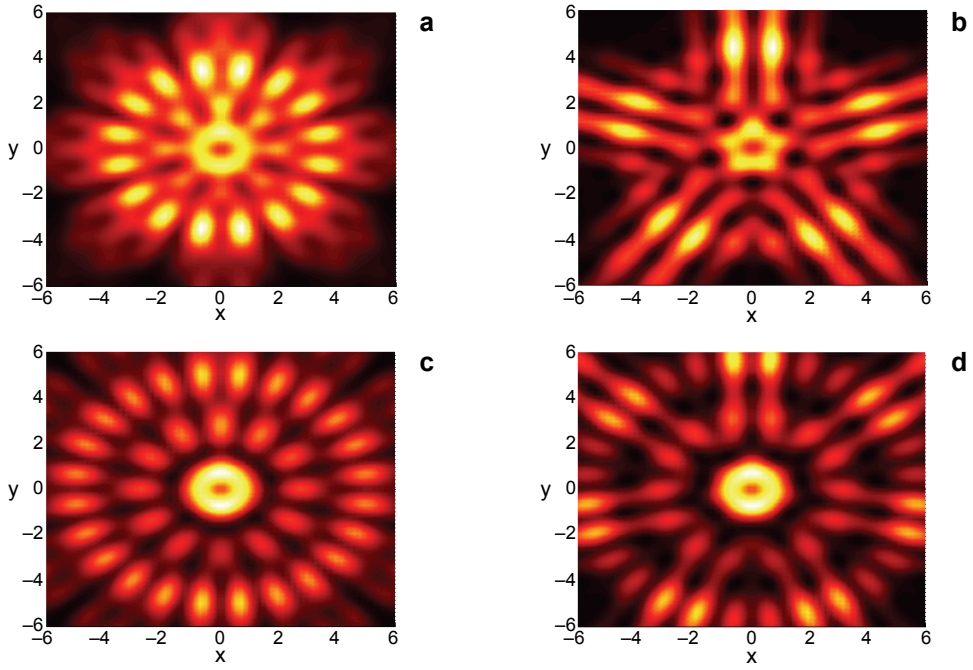
Fig. 7. Intensity distributions for $\beta_1 = 0.2$, NA = 0.5, and $m = 4$ (**a**), $m = 5$ (**b**), $m = 6$ (**c**), $m = 7$ (**d**).
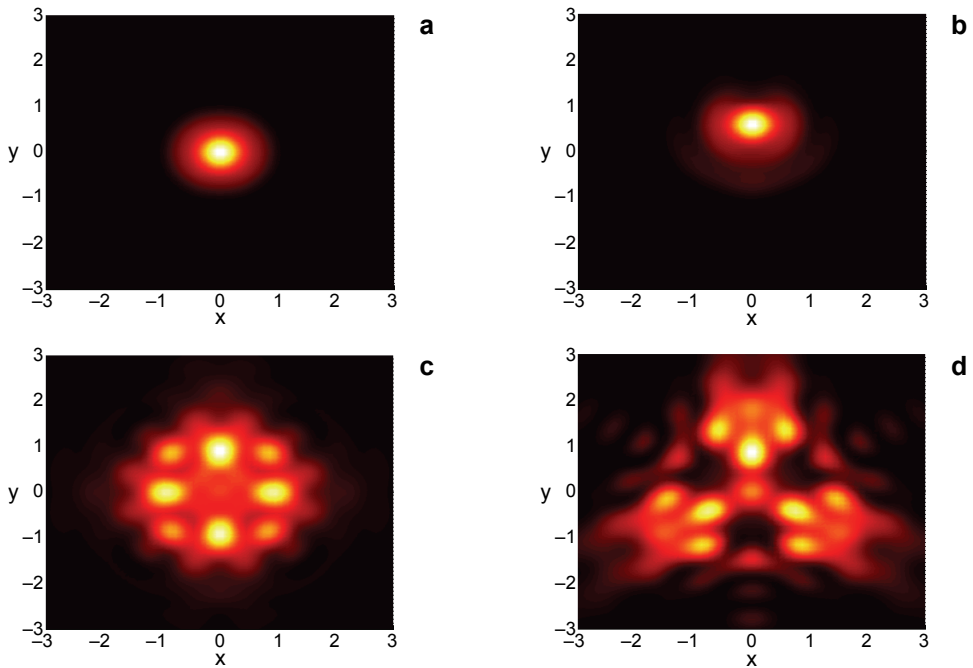


Fig. 8. Intensity distributions for $\beta_1 = 1$, NA = 0.95, and $m = 0$ (**a**), $m = 1$ (**b**), $m = 2$ (**c**), $m = 3$ (**d**).
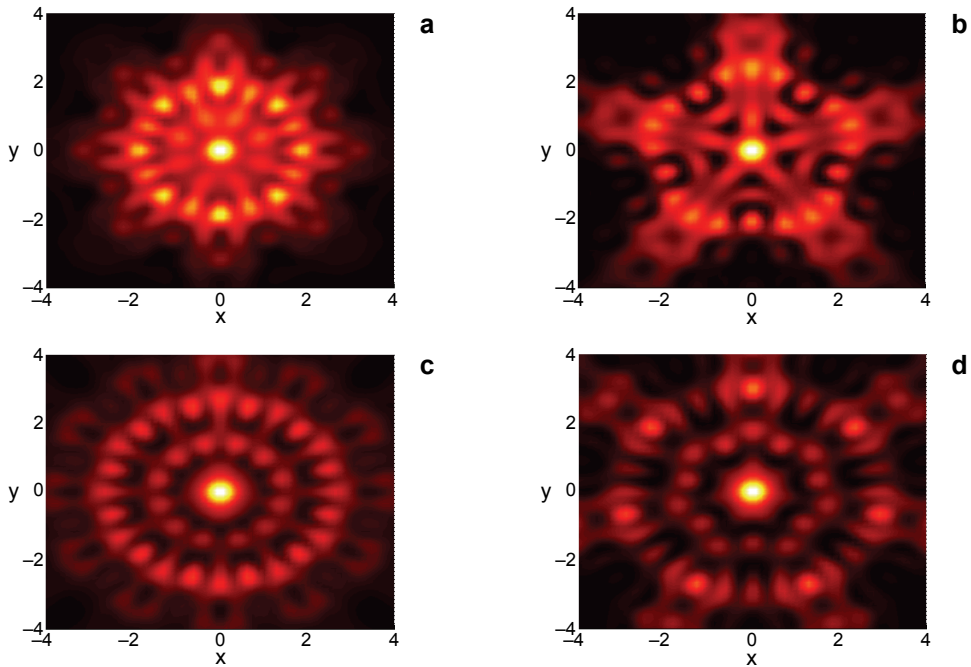
Fig. 9. Intensity distributions for $\beta_1 = 1$, NA = 0.95, and $m = 4$ (**a**), $m = 5$ (**b**), $m = 6$ (**c**), $m = 7$ (**d**).

pentagon pattern, as shown in Fig. 9**b**. Moreover, each reduplicate intensity element consists of multiple intensity peaks. For a higher phase parameter, the whole focal pattern turns on an intensity peak wheel, which is very symmetric. From the above focal pattern evolution process it can be seen that when the phase parameter is an odd number, the number of reduplicate intensity elements is equal to the phase parameter. However, when the phase parameter is an even number, the number of reduplicate intensity elements is twice the phase parameter. Therefore, there is a clear relation between the focal pattern and the phase parameter.

When the Bessel beam parameter increases as $\beta_1 = 2$ under condition of NA = 0.95, the focal pattern evolution on an increasing phase parameter is also studied. Figures 10 and 11 give the focal patterns for $\beta_1 = 2$, NA = 0.95, and different phase parameters $m$. By comparing Figs. 10 with 8, it can be seen that the effect of $\beta_1$ on the focal pattern is very considerable. Without any wavefront phase modulation, the focal spot extends remarkably under condition $\beta_1 = 2$. And the focal spot changes into one crescent shape for $m = 1$, as shown in Fig. 10**b**. For case of $m = 2$, there are four overlapping intensity peaks with five weak dark hollow foci, as illustrated in Fig. 10**c**, which differs remarkably from the focal pattern under condition of $\beta_1 = 1$ that is shown in Fig. 8**c**. When $m$ increases to 3, the reduplicate intensity element changes very considerably though the whole focal pattern turns on a triangle shape by comparing Figs. 10**d** with 8**d**. From the above focal pattern evolution process, we can see that the effect of the Bessel beam parameter on the focal pattern is very remarkable under
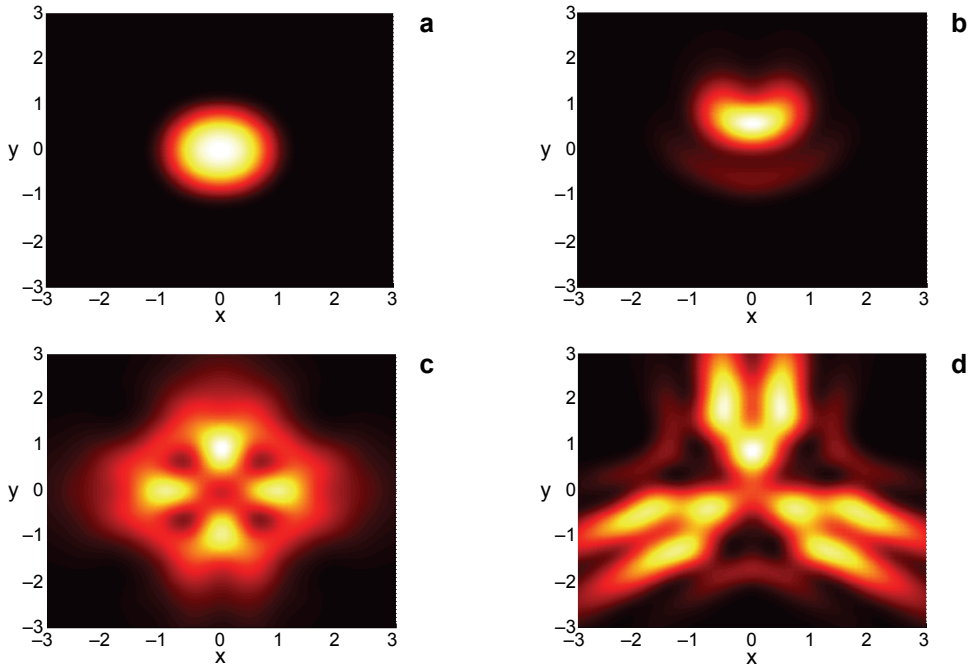
Fig. 10. Intensity distributions for $\beta_1 = 2$, NA = 0.95, and $m = 0$ (**a**), $m = 1$ (**b**), $m = 2$ (**c**), $m = 3$ (**d**).
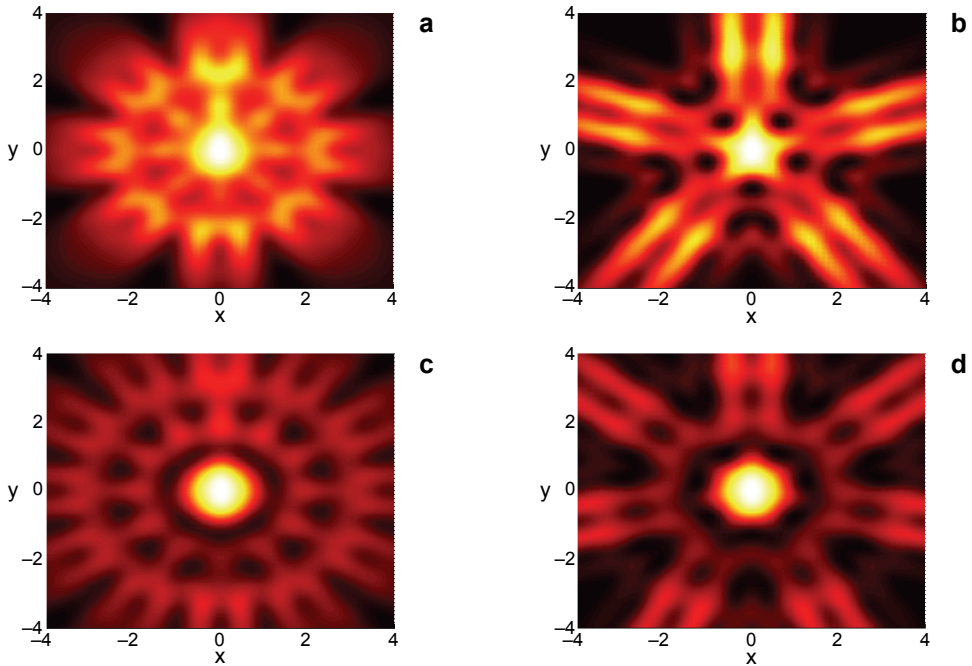


Fig. 11. Intensity distributions for $\beta_1 = 2$, NA = 0.95, and $m = 4$ (**a**), $m = 5$ (**b**), $m = 6$ (**c**), $m = 7$ (**d**).

the condition of a higher numerical system, which is different from that for case of low numerical aperture. By comparing Figs. 11 with 9, we can also see that the effect of the Bessel beam parameter on the focal pattern lies in the shape of a reduplicate intensity element. In fact, the symmetry properties of the whole focal pattern do not change, *i.e.*, the relation of the number of reduplicate intensity elements and phase parameters is the same. Namely, for a higher phase parameter, the whole focal pattern turns on an intensity peak wheel, which is very symmetric, and when the phase parameter is an odd number, the number of reduplicate intensity elements is equal to the phase parameter. However, when the phase parameter is an even number, the number of reduplicate intensity elements is twice the phase parameter.

Though this manuscript is aiming at investigating theoretically the focusing properties of the radially polarized Bessel–Gauss beam with a sine-azimuthal variation wavefront, we want to show some description of the realization of the proposed concept. There are two main aspects related to the experiment. Firstly, the radially polarized Bessel–Gauss beam with a sine-azimuthal variation wavefront should be obtained experimentally. In fact, many methods have been proposed to generate a vector beam, including radially polarized beams, which may be classified as intra-cavity methods and external conversion methods [26–28]. The intra-cavity method is carried out by placing designed optical elements inside the laser cavity or designing a special cavity. For instance, AHMED *et al*. reported on the highly efficient intra-cavity generation of beams with radial polarization in an Yb:YAG thin-disk laser, in which an intra-cavity circular resonant waveguide grating was used as a polarization selective mirror inside the laser cavity [29]. In addition, a photonic crystal mirror with polarization selectivity was also used for the generation of radially polarized beams from an Nd:YAG laser cavity [30, 31]. The external conversion method uses polarization converters outside the laser cavity. Setups with a radial analyzer made either of birefringent materials [32] or of dichroic materials [33] can be used to generate the cylindrical vector beam. Another kind of method for generating cylindrical vector beams is based on a liquid crystal spatial light modulator or diffractive phase element [34, 35]. Some external conversion methods use interference optical systems [36, 37]. We plan to construct a radially polarized beam by an interference optical system, where the amplitude and wavefront phase distributions for generating the radially polarized Bessel–Gauss beam with a sine-azimuthal variation wavefront will be obtained by the amplitude and phase spatial light modulators. We have bought these two kinds of spatial light modulators from Holoeye Inc. for experimental researches. The second aspect related to the experiment is to measure intensity distribution in the focal region with nanometer resolution. The test principle in a scanning near-field optical microscope can be employed here. A single mode optical fiber probe can be used for scanning the optical field with three-dimensional nanometer resolution, and the optical signal is transformed to the electric signal simultaneously, so that intensity distribution can be obtained even when the numerical aperture is very high. Experimental researches of focusing properties of many novel beams are our next step stage; we are preparing to construct the experimental system.

# 4. Conclusions

Focusing of the radially polarized Bessel–Gauss beam with a sine-azimuthal variation wavefront was investigated by the vector diffraction theory. Wavefront distribution is the sine function of the azimuthal angle with one phase parameter that indicates the phase change frequency. It was found that the focal pattern can be altered by the phase parameter remarkably, and many novel focal patterns may occur. For case of a higher phase beam, the whole focal pattern turns on a symmetric wheel shape with multiple reduplicate intensity elements. And there is a clear relation between the focal pattern and the phase parameter. When the phase parameter is an odd number, the number of reduplicate elements is equal to the phase parameter. However, when the phase parameter is an even number, the number of reduplicate elements is twice the phase parameter. What is more interesting, the effect of a phase parameter on the focal pattern is more considerable than that of a beam parameter under low numerical aperture. Under higher numerical aperture, the effect of a beam parameter on the focal pattern gets stronger. The focal pattern evolution of this kind of the radially polarized Bessel–Gauss beam may find applications in many domains, such as optical machining, optical tweezers, and multifoci microscopy.

# References

[1] Durnin J., *Exact solution for nondiffracting beams. I. The scalar theory*, Journal of the Optical Society of America A **4**(4),1987, pp. 651–654.

[2] Bouchal Z., Olivik M., *Non-diffractive vector Bessel beams*, Journal of Modern Optics **42**(8), 1995, pp. 1555–1566.

[3] Garcés-Chávez V., McGloin D., Melville H., Sibbett W., Dholakia K., *Simultaneous micromanipulation in multiple planes using a self-reconstructing light beam*, Nature **419**, 2002, pp. 145–147.

[4] Jarutis V., Matijošius A., Di Trapani P., Piskarskas A., *Spiraling zero-order Bessel beam*, Optics Letters **34**(14), 2009, pp. 2129–2131.

[5] Vysa S., Kozawa Y., Sato S., *Self-healing of tightly focused scalar and vector Bessel–Gauss beams at the focal plane*, Journal of the Optical Society of America A **28**(5), 2011, pp. 837–843.

[6] Gori F., Guattari G., Padovani C., *Bessel–Gauss beams*, Optics Communications **64**(6), 1987, pp. 491–495.

[7] Seshadri S.R., *Virtual source for the Bessel–Gauss beam*, Optics Letters **27**(12), 2002, pp. 998–1000.

[8] April A., *Bessel–Gauss beams as rigorous solutions of the Helmholtz equation*, Journal of the Optical Society of America A **28**(10), 2011, pp. 2100–2107.

[9] Bagini V., Frezza F., Santarsiero M., Schettini G., Schirripa Spagnolo G., *Generalized Bessel––Gauss beams*, Journal of Modern Optics **43**(6), 1996, pp. 1155–1166.

[10] JORDAN R.H., HALL D.G., *Free-space azimuthal paraxial wave equation: the azimuthal Bessel––Gauss beam solution*, Optics Letters **19**(7), 1994, pp. 427–429.
[11] GREENE P.L., HALL D.G., *Diffraction characteristics of the azimuthal Bessel–Gauss beam*, Journal of the Optical Society of America A **13**(5), 1996, pp. 962–966.
[12] CHEN J., YU Y., *The focusing property of vector Bessel–Gauss beams by a high numerical aperture objective*, Optics Communications **283**(9), 2010, pp. 1655–1660.
[13] ITO A., KOZAWA Y., SATO S., *Generation of hollow scalar and vector beams using a spot-defect mirror*, Journal of the Optical Society of America A **27**(9), 2010, pp. 2072–2077.
[14] WANG H., SHI L., LUKYANCHUK B., SHEPPARD C., CHONG C.T., *Creation of a needle of longitudinally polarized light in vacuum using binary optics*, Nature Photonics **2**(8), 2008, pp. 501–505.
[15] HUANG K., SHI P., KANG X.L., ZHANG X., LI Y.P., *Design of DOE for generating a needle of a strong longitudinally polarized field*, Optics Letters **35**(7), 2010, pp. 965–967.
[16] YEW E.Y.S., SHEPPARD C.J.R., *Tight focusing of radially polarized Gaussian and Bessel–Gauss beams*, Optics Letters **32**(23), 2007, pp. 3417–3419.
[17] HUANG K., SHI P., CAO G.W., LI K., ZHANG X.B., LI Y.P., *Vector-vortex Bessel–Gauss beams and their tightly focusing properties*, Optics Letters **36**(6), 2011, pp. 888–890.
[18] LEDESMA S., CAMPOS J., ESCALERA J.C., YZUEL M.J., *Symmetry properties with pupil phase-filter*, Optics Express **12**(11), 2004, pp. 2548–2559.
[19] WANG H., GAN F., *High focal depth with a pure-phase apodizer*, Applied Optics **40**(31), 2001, pp. 5658–5662.
[20] DE JUANA D.M., CANALES V.F., VALLE P.J., CAGIGAL M.P., *Focusing properties of annular binary phase filters*, Optics Communications **229**(1–6), 2004, pp. 71–77.
[21] CANALES V.F., OTI J.E., CAGIGAL M.P., *Three-dimensional control of the focal light intensity distribution by analytically designed phase masks*, Optics Communications **247**(1–3), 2005, pp. 11–18.
[22] GAO X., GAN F., XU W., *Superresolution by three-zone pure phase plate with 0, π, 0 phase variation*, Optics and Laser Technology **39**(5), 2007, pp. 1074–1080.
[23] SATO S., KOZAWA Y., *Hollow vortex beams*, Journal of the Optical Society of America A **26**(1), 2009, pp. 142–146.
[24] YOUNGWORTH K.S., BROWN T.G., *Focusing of high numerical aperture cylindrical-vector beams*, Optics Express **7**(2), 2000, pp. 77–87.
[25] VISSCHER K., BRAKENHOFF G.J., *Theoretical study of optically induced forces on spherical particles in a single beam trap I: Rayleigh scatterers*, Optik **89**, 1992, pp. 174–180.
[26] MOSHE I., JACKEL S., MEIR A., *Production of radially or azimuthally polarized beams in solid-state lasers and the elimination of thermally induced birefringence effects*, Optics Letters **28**(10), 2003, pp. 807–809.
[27] BISSON J.-F., LI J., UEDA K., SENATSKY YU., *Radially polarized ring and arc beams of a neodymium laser with an intra-cavity axicon*, Optics Express **14**(8), 2006, pp. 3304–3311.
[28] YONEZAWA K., KOZAWA Y., SATO S., *Generation of a radially polarized laser beam by use of the birefringence of a* c-*cut Nd:YVO$_4$ crystal*, Optics Letters **31**(14), 2006, pp. 2151–2153.
[29] AHMED M.A, HAEFNER M., VOGEL M., PRUSS C., VOSS A., OSTEN W., GRAF T., *High-power radially polarized Yb:YAG thin-disk laser with high efficiency*, Optics Express **19**(6), 2011, pp. 5093–5103.
[30] NODA S., YOKOYAMA M., IMADA M., CHUTINAN A., MOCHIZUKI M., *Polarization mode control of two-dimensional photonic crystal laser by unit cell structure design*, Science **293**(5532), 2001, pp. 1123–1125.
[31] IWAHASHI S., KUROSAKA Y., SAKAI K., KITAMURA K., TAKAYAMA N., NODA S., *Higher-order vector beams produced by photonic-crystal laser*, Optics Express **19**(13), 2011, pp. 11963–11968.
[32] ZHAN Q., LEGER J.R., *Microellipsometer with radial symmetry*, Applied Optics **41**(22), 2002, pp. 4630–4637.

[33] ZHAN Q., LEGER J.R., *Interferometric measurement of the geometric phase in space-variant polarization manipulations*, Optics Communications **213**(4–6), 2002, pp. 241–245.
[34] STALDER M., SCHADT M., *Linearly polarized light with axial symmetry generated by liquid crystal polarization converters*, Optics Letters **21**(23), 1996, pp. 1948–1950.
[35] NIU C.-H., GU B.-Y., DONG B.-Z., ZHANG Y., *A new method for generating axially-symmetric and radially-polarized beams*, Journal of Physics D: Applied Physics **38**(6), 2005, pp. 827–832.
[36] TIDWELL S.C., KIM G.H., KIMURA W.D., *Efficient radially polarized laser beam generation with a double interferometer*, Applied Optics **32**(27), 1993, pp. 5222–5229.
[37] PASSILLY N., DE SAINT DENIS R., AIT-AMEUR K., TREUSSART F., HIERLE R., ROCH J.-F., *Simple interferometric technique for generation of a radially polarized light beam*, Journal of the Optical Society of America A **22**(5), 2005, pp. 984–991.